Regional glucose hypometabolic spread within the primary motor cortex is associated with amyotrophic lateral sclerosis disease progression: A fluoro-deoxyglucose positron emission tomography study

Hironobu Endo, Kenji Sekiguchi *, Takehiro Ueda, Hisatomo Kowa, Fumio Kanda, Tatsushi Toda

Division of Neurology, Kobe University Graduate School of Medicine, Kobe City, Japan

ARTICLE INFO

ABSTRACT

Objective: Here we investigate the process of neurodegeneration in amyotrophic lateral sclerosis (ALS). The relationship between the cortical field spreading of glucose metabolic decreases in the primary motor cortex (PMC) and the progression of corresponding extremity dysfunction was evaluated using [18F] fluoro-deoxyglucose (FDG)-positron emission tomography (PET).
Methods: Patients with ALS underwent [18F] FDG-PET and the resulting datasets were individually contrasted against healthy controls using the NEUROSTAT software. The extent ratio was defined as the proportion of pixels with a significant Z-score decrease within regions of the primary motor cortex (precentral gyrus or paracentral lobule) opposite to the impaired upper extremities (UEs) or lower extremities (LEs), respectively. Clinical symptoms in all extremities were assessed using an upper motor neuron (UMN) score and the MRC (Medical Research Council) sum score upon physical examination. Cross-sectional correlations were analysed between clinical symptoms, the duration of these symptoms, and the extent ratio.
Results: Nineteen regions of the primary motor cortex corresponding to symptomatic limb in 10 participants were evaluated. In the corresponding region of the primary motor cortex, the extent ratio increased (same meaning as hypometabolic area spread) in association with symptom duration ($r_s = 0.5$, $p = 0.03$). Neither UMN nor lower motor neuron (LMN) scores were correlated with symptom duration. Three out of 19 impaired regions did not show upper motor neuron (UMN) signs upon physical examination. The extent ratio and UMN score-controlled symptom duration were partially correlated ($r_s = 0.5$, $p = 0.05$).
Conclusions: In patients with ALS, glucose metabolism decreased in the impaired side of the primary motor cortex depending on the clinical symptom progression in the corresponding extremities, regardless of the presence of clinical UMN signs. A decrement in glucose metabolism on FDG-PET corresponding to symptoms in the primary motor cortex might be an indicator of the time-dependent course of ALS neurodegeneration.

1. Introduction

The natural progression of motor neuron degeneration in amyotrophic lateral sclerosis (ALS), identified in 1874 by Charcot [1], is not clearly understood. ALS features a variety of heterogeneous motor phenotypes that are likely due to the contiguous but independent spread of pathophysiology through the upper (UMN) and lower motor neurons (LMN) [2]. At the UMN level, focal degeneration spreads to the medial-lateral ipsilateral side during the primary phase, and subsequently to the contralateral side during the advanced phase.

Recently, the time-dependent propagation of phosphorylated TDP-43 aggregates, a pathological hallmark of ALS, was identified in an autopsy study [3]. In addition, an *in vitro* study demonstrated that insoluble TDP-43 prepared from ALS brains acted as a seed-dependent aggregator of TDP-43 [4]. On a pathological level, these reports support Ravits' spreading theory [2]. Clinically, however, the spreading and propagation hypotheses have yet to be clearly verified, especially with regard to UMN degeneration [5].

Clinical signs and functional imaging, which often reflect changes in disease progression, provide a significant contribution to the understanding of UMN pathophysiology in ALS. Previous studies of functional brain imaging in ALS have reported decreased cerebral perfusion or glucose metabolism [6,7]. [18F] fluoro-deoxyglucose-positron emission tomography (FDG-PET) studies also report that the cerebral metabolic rate of glucose consumption was significantly lower in patients with ALS than in healthy controls [8]. Moreover,

* Corresponding author at: Division of Neurology, Kobe University Graduate School of Medicine, 7-5-2, Kusunoki-cho, Chuo-ku, Kobe City, Hyogo 650-0017, Japan.
E-mail address: sekiguch@med.kobe-u.ac.jp (K. Sekiguchi).
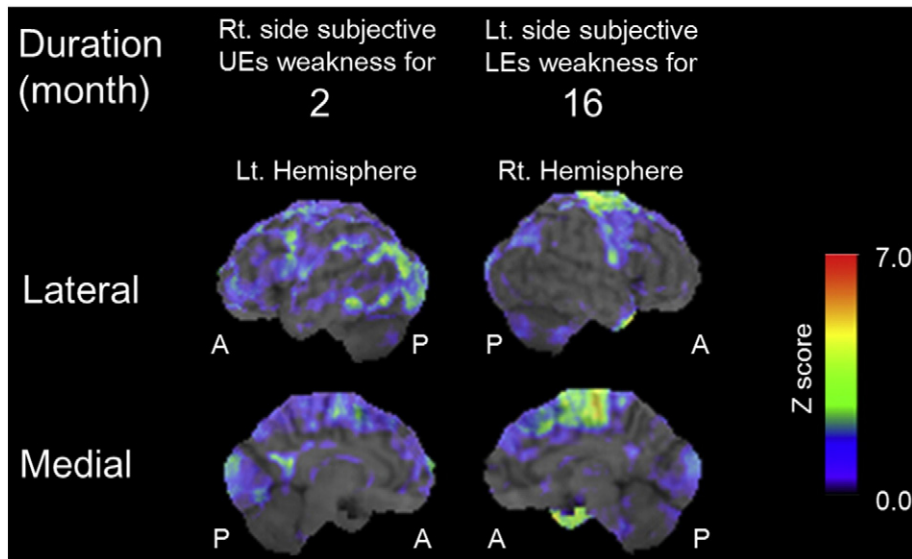
Fig. 1. Representative images of decreased Z-score > 1.5 maps in patients. Z-score maps merged with standardized MRI. There is no significant hypometabolic region on the left precentral gyrus opposite to right upper extremity started weakness 2 months before (left column, case 1). There is expanded hypometabolic region on the right precentral gyrus and paracentral lobule corresponding to weak left lower extremity for 16 months (right column, case 7). Abbreviations: A, Anterior; Lt, Left; LEs, Lower extremities; P, Posterior; Rt, Right; UEs, Upper extremities.

regional cerebral hyper-glucose metabolism in ALS was recently reported based on FDG-PET analysis; this finding could be due to the local activation of astrocytes and microglia [9,10]. Thus, the results of FDG-PET analysis in patients with ALS are still controversial.

However, as aforementioned, the impaired cerebral region and the extent of functional impairment might vary during disease progression in patients with ALS, and even between patients due to clinical diversity. Cerebral functional imaging studies have considered the clinical profiles of participants at inclusion, but not the rate of disease progression or the location of injury in the brain.

Time-dependent changes in glucose metabolism within the impaired primary motor cortex (PMC) should be considered because regional changes in glucose metabolism during disease progression might reflect the spread of UMN neurodegeneration, including neuronal dysfunction and cell death. We hypothesize that decreases in glucose metabolism corresponding to symptoms in the PMC might be an indicator of the time-dependent course of ALS neurodegeneration. In the present study, we aimed to improve the understanding of UMN neurodegeneration in patients with ALS through investigating the relationship between glucose metabolism in the impaired hemisphere of the motor cortex and the time from symptom onset.
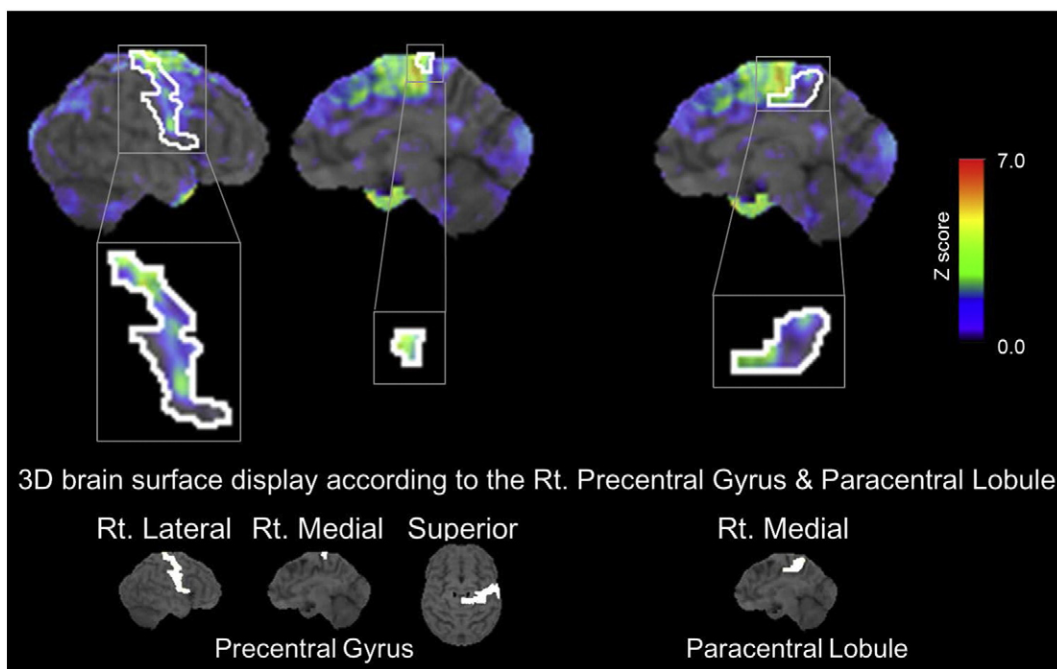
Fig. 2. Upper panel shows the decreased Z-score > 1.5 map of right lateral side and medial side merged with precentral gyrus (left, middle, respectively) or paracentral lobule (right) coordinates and standardized MRI. Lower panel shows extracted coordinates of precentral gyrus and paracentral lobule according to the Talairach daemon coordinates. Abbreviations: 3D, three-dimension; PCG, precentral gyrus; PCL, paracentral lobule; Rt., Right.

2. Methods

2.1. Participants

Ten patients diagnosed with possible, probable, and definite ALS according to the revised El Escorial criteria [11] who underwent whole body FDG-PET to rule out paraneoplastic motor neuron disease between January 2008 and August 2016 were retrospectively recruited for the present study. The cross-sectional relationship between glucose metabolism in the impaired hemisphere of the motor cortex and persistent symptom duration in each patient was investigated using FDG-PET. Symptom duration was defined as the number of months from symptom onset to the date of PET scanning. Symptom onset was defined as the point at which the patient became aware of weakness or clumsiness in the upper extremities (UEs) and lower extremities (LEs), based on medical records. The side of symptom onset was recorded in each patient as the laterality specific disease duration.

To reduce disease heterogeneity, we excluded from our analysis, three patients with frontal lobe dementia (clinically obvious disinhibition, character change, apathy, or aphasia), one patient with multiple cerebral infarctions, and one patient with cervical myelopathy.

None of the patients with ALS required assisted ventilation. However, some concurrent conditions were present, including hypertension, dyslipidaemia, ulcerative colitis, or benign prostate hypertrophy. The ethical committees of the Kobe University Graduate School of Medicine approved our study.

2.2. Clinical assessment

All clinical assessments were evaluated within one month from the FDG-PET scan. An in-house-adapted version of a UMN score was based on the following neurologic signs: for UEs, the biceps reflex, triceps reflex, brachioradialis reflex, finger jerks, and Hoffmann's sign; for LEs, the patellar tendon reflex, Achilles tendon reflex, Babinski reflex, Chaddock reflex, and leg spasticity in reference to previous report [12, 13]. The score ranged from 0 to 20 (each parts of the maximum UMN score = 5). Sub-score range was 0 = absence or normal to 1 = impaired or hyperactive. Regions with muscle atrophy or weakness that showed a normal muscle tendon reflex were judged as hyperactive.

The LMN disease burden was measured according to the MRC (Medical Research Council) scale from 0 (no movement) to 5 (full strength) in the following regions: for UEs, the deltoid, biceps brachii, triceps brachii, wrist extension, wrist flexion, finger extension, and finger abduction; for LEs, the Iliopsoas, quadriceps, hamstrings, tibialis anterior, gastrocnemius, extensor hallucal longus, and flexor hallucal longus. The score ranged from 0 to 140 (each parts of the maximum MRC score = 35).

2.3. FDG-PET study

Prior to radiopharmaceutical injection, patients fasted for at least 6 h. Blood glucose was approximately 200 mg/dl or less in all patients, who then received an intravenous injection of 256 ± 48 MBq (mean $\pm$ SD) of FDG. Approximately 60 min after FDG injection, PET scanning was performed. Thirteen patient images were acquired using a commercially available PET system (Philips Allegro, Philips Healthcare, Best, Netherlands). After positioning the patient, a static emission scan was performed with 2 to 2.5 min of acquisition in each bed position, spanning from the upper thigh to the top of the skull with a total of 9–10 bed positions. Transmission was performed using a ^{137}Cs ring for 25 s per bed position. PET data were acquired in 3D mode and images were reconstructed using an ordered-subset expectation maximization iterative reconstruction algorithm (RAMLA). The field of view and pixel size of the reconstructed images were 57.6 cm and 4.0 mm, respectively, with a matrix size of 144×144 mm.

Table 1
Basic patient characteristics and demographics.

Case	Age	Gender	Duration (month)	Impaired region number	First symptom	Following symptoms	Rt UE UMN score	Lt UE UMN score	Rt LE UMN score	Lt LE UMN score	Rt UE MRC score	Lt UE MRC score	Rt LE MRC score	Lt LE MRC score	Rt PCG extent ratio Z > 1.5	Lt PCG extent ratio Z > 1.5	Rt PCL extent ratio Z > 1.5	Lt PCL extent ratio Z > 1.5	Revised El Escorial clinical classification
1	54	M	2	1	Rt UE	Bulbar	4				27					13			Probable
2	55	M	1	2	Lt LE			0		3		26		27	7		0		Definite
3	56	M	4	3	Lt UE	Lt LE		0				28					23		Possible
			11	4									31						
			6	5														2	
4	62	M	1	6	Lt UE	Rt UE	3	2			25	25			11	26			Definite
5	60	M	8	7	Rt UE	Lt UE, Bulbar	3	0			25	26			0	8			Probable
			4	8															
			11	9															
6	43	F	2	10	Rt LE	Rt UE, Bulbar	1		2	4	32		30	23		0		26	Possible
			5	11													31		
7	70	F	2	12	Lt LE	Lt UE		5		4		27		23	32				Possible
			16	13				4				29			20				
8	69	F	5	14	Lt UE	Rt UE	5	5			32	21			4	18			Possible
			12	15															
9	73	F	3	16	Lt UE, Bulbar	Rt UE	5				23					3			Definite
			11																
10	63	M	2	17	Rt LE	Lt LE			4	3			31	32	0		0	45	Definite
			8	18															
			3	19															

Abbreviations: F, Female; LE, Lower extremity; Lt, Left; M, male; MRC Medical Research Council; PCG, precentral gyrus; PCL paracentral lobule; Rt, Right; UE, Upper extremity; UMN, Upper motor neuron.

2.4. Data analysis

Each dataset was analysed using the three-dimensional stereotactic surface projection (3D-SSP) program of the NEUROSTAT software [14]. This analysis enabled the minimization of anatomic variation across patients while preserving regional metabolic activity and comparison on a pixel-by-pixel basis. The original PET image set was resampled into a standard stereotactic image format. For this process, an automated algorithm was used to estimate the location of the line spanning from the anterior commissure to the lower border of the posterior commissure (AC-PC) on a PET mid-sagittal plane and to realign image data to the standard stereotactic orientation [15,16]. Regions showing an anatomical difference in individual brain structures between the PET image data and a standard brain atlas were minimized using linear scaling and nonlinear warpping techniques [17].

2.5. Normal reference database

The normative FDG-PET database from Iseki et al. was used as a normal reference database in the present study [18]. This data set consisted of three age groups (40–64 y, 65–74 y, and above 75 y) of 77 normal Japanese volunteers from 41 to 84 years of age (36 men and 41 women) who underwent clinical, neuropsychological, and MRI examinations. All 77 subjects met the inclusion criteria with regard to educational background, past medical history, and neuropsychological examination. In addition, MRI was used to evaluate brain atrophy and vascular changes in relation to age (1.5T scanner, Magnetom Symphony, Siemens, Erlangen, Germany). The PET scanner used was a Discovery ST (General Electric Healthcare, Waukesha, WI, USA). Approximately 40–60 min after intravenous administration of 185 MBq/2 ml of FDG, PET images were obtained using the standard 3D emission scan mode. The duration of scanning was 15 min. The matrix size was 128×128 mm.

2.6. Data extraction for cerebral glucose metabolic activity

To evaluate changes in the regional normalized cerebral metabolic rate of glucose (CMRglc) in patients with ALS at the same pixel coordinates, a set of surface pixels from each patient was compared against the age matched group of a normal database, as mentioned above, using 3D-SSP analysis. After anatomical standardization for each predetermined surface pixel, the algorithm searched for the highest pixel value in an inward direction along the vector to a six-pixel depth into the cortex. The maximum values were then projected to the surface on a pixel-by-pixel basis.

2.7. Calculation of individual Z-score data

The regional Z-score was determined using the stereotactic extraction estimation (SEE) method developed by Mizumura et al. [19], which measures the Z-score association between the patient's coordinates and the coordinates in the prepared reference from the Talairach daemon [20]. Decreases in the CMRglc were expressed as a Z-score map, which was generated for each individual pixel in the 3D-SSP format as follows: Z-score = ([normal mean] − [individual patient value]) / (normal SD).

Each Z-score map was normalized by the whole brain average count derived from all patients with ALS. Significantly decreased regions of glucose metabolism in precentral gyrus (PCG) and paracentral lobule (PCL) coordinates were determined as extent ratios for individual patient PET scans with a threshold Z-score of >1.5 [21]. For each patient with ALS, a Z-score was calculated corresponding to the three age groups of the normal patient data (40–64 y, 65–74 y, and above 75 y). Subsequently, the percentage of pixels exceeding a threshold in the brain surface display according to the Talairach daemon PCG and PCL coordinates. The extent ratios were calculated independently for each hemisphere. We defined PCG coordinates corresponding to upper extremities symptoms and PCL coordinates corresponding to lower extremities symptoms [22]. We visually checked whether a minor involvement could be observed for the dorsal side of the PCL, which is includes a sensory area.

Extent ratios (the population of the pixels with a Z-score > 1.5) were calculated as: Decreased pixel numbers in the PCG or PCL coordinates (Z-score > 1.5) / total pixel numbers of the PCG or PCL coordinates × 100.

A representative Z-score map for patients with ALS is displayed on a standardized MRI image (Fig. 1). Fig. 2 shows the PCG and PCL coordinates, and regions in those areas with a decreased Z-score.

2.8. Statistical analysis

The Spearman's rho correlation test was used for correlation analysis. A partial correlation was also analysed using a nonparametric test. All statistical analyses were performed using IBM SPSS Statistics software (version 22, IBM, Armonk, NY). Results with p-values ≤ 0.05 were considered significant.

3. Results

3.1. Baseline characteristics

The ten patients with ALS had a mean age of 60.5 ± 9.0 years old, and included four females and nine males. Impaired hemisphere regions were defined based on the medical records that indicated when the patient became aware of weakness or clumsiness in extremities, the PCG coordinates corresponding to upper extremities symptoms, and the PCL coordinates corresponding to lower extremities symptoms. The total number of impaired hemisphere regions was 19, and the mean symptom duration for the analysed hemisphere was 6.1 ± 4.3 months (overall disease duration of 8.8 ± 4.2 months). Bulbar only onset of
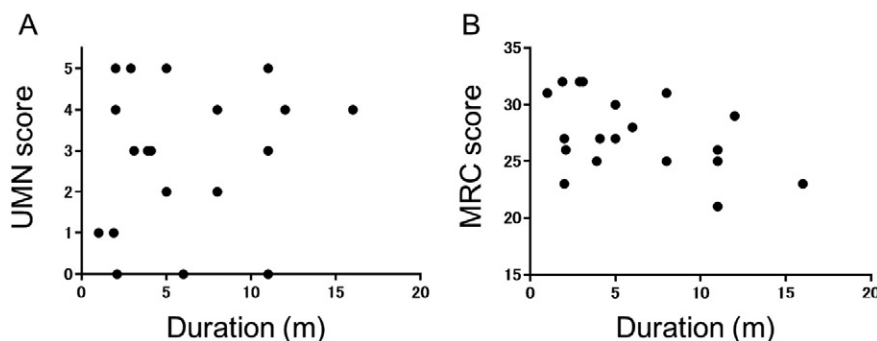
Fig. 3. A: Scatter plots of upper motor neuron (UMN) scores of corresponding brain regions associated with patient symptoms and the symptom duration. B: Scatter plots of Medical Research Council (MRC) scores of the corresponding brain regions associated with patient symptoms and the symptom duration.
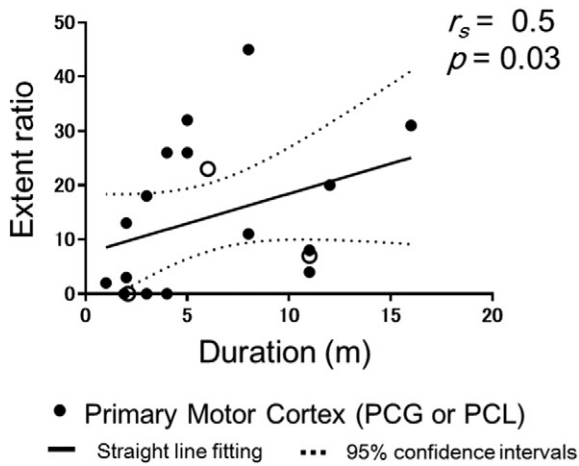
Fig. 4. Scatter plots of extent ratio Z-scores > 1.5 for the symptomatic primary motor cortex regions (the precentral gyrus for upper extremities symptoms or the paracentral lobule for lower extremities symptom) against symptom duration. Open circle showed the impaired regions with UMN score = 0. The straight line (Liner regression) and dotted line (95% confidence intervals) are derived from a regression analysis.

the first symptom was not observed in our study. Other symptoms and clinical data are shown in Table 1.

Both UMN scores and MRC scores in the 19 symptomatic regions were not correlated with symptom duration ($r_s = 0.2$, $p = 0.60$ and $r_s = -0.4$, $p = 0.10$, respectively) (Fig. 3A and B).

3.2. Glucose hypometabolism spread in a region of the PMC along with a corresponding persistent duration of symptoms

Nineteen symptomatic regions were identified that corresponded to the extremities of ten patients (Table 1). The extent ratio (percentage decrease) in the symptomatic region of the PCG or PCL with a Z-score > 1.5 correlated with symptom duration ($r_s = 0.5$, $p = 0.03$) (Fig. 4). Three out of 19 impaired regions never showed simultaneous upper motor neuron (UMN) signs upon physical examination. Neither the extent ratio nor the LMN scores correlated with the corresponding side of UMN ($r_s = 0.3$, $p = 0.20$, $r_s = -0.1$, $p = 0.80$) (Fig. 5). In order to exclude partial effect of UMN symptoms, we also analysed partial correlation. The extent ratio was partially correlated with symptom duration after controlling for the UMN score ($r_s = 0.5$, $p = 0.05$). The dorsal region of the PCL, which is a sensory area, showed no involvement based on a visual inspection.

4. Discussion

The present study demonstrates the relationship between cerebral glucose metabolism in the PMC (PCG and PCL) and a corresponding

persistent duration of symptoms in disturbed limbs, as well as the UMN burden in patients with ALS. These results show that the lesions continuously spread in the brain area where the initial symptoms appeared, suggesting that areas of glucose hypometabolism spread within the PMC could indicate disease progression, consistent with Ravits' spreading theory [2]. Our data suggest that symptom duration has a greater influence on the regional decrease in cerebral glucose metabolism within PMC than UMN scores.

Lesions of glucose hypometabolism begin to spread gradually in the diseased PCG and PCL during disease progression, reflecting neuronal dysfunction and cell death in the PMC [22,23]. Our results are consistent with those of previous studies that reported significantly lower rates of cerebral metabolic glucose consumption in the frontal lobe of patients with ALS compared to healthy controls [8,24]. However, fronto-temporal lobar degeneration (FTLD) with motor neuron disease has been recognized since 1994 [25]. Van Laere et al. recently demonstrated the presence of glucose hypometabolism in prefrontal area in a large prospective PET study of patients with ALS [26]. The findings of their study, however, do not exclude patients with FTLD-ALS. In our study, patients with FTD were excluded from the data analysis. Moreover different from their case-control comparison, we have focused on the relationship between focal changes only in the PMC and impaired duration of the corresponding extremities for each participants.

The present study predominantly focused on the precentral cortex of the PMC, but not the Brodmann areas 4 (BA4) or premotor cortex. The PMC is analogous to BA4, as the premotor cortex is analogous to BA6, 8 and 9. On the 3D-SSP surface maps, the number of coordinates where anatomical information was obtained by BA and gyrus area was approximately 40% and 80%, respectively [19]. Thus, we evaluated the precentral cortex (PCG and PCL) to focus on an area with the sufficient amount coordinate [19]. In spinal-bulbar muscular atrophy (SBMA) glucose hypometabolism lesions can also be detected in the premotor cortex of the frontal lobe (BA6, 8, and 9, but not BA4) [27]. SMBA is a hereditary, progressive LMN disease, where neurons in the PMC are typically preserved [28]. In the present study, the extension of PMC glucose hypometabolism lesions might influence functional hypometabolism not only *via* lower motor neuron dysfunction but also *via* neuronal cell loss in the PMC.

During disease progression, the glucose hypometabolism lesions spread within the PMC regardless of the UMN clinical signs. Thus, our results suggest that FDG-PET could more accurately identify UMN impairments compared to the UMN clinical signs. This finding was the result of LMN signs masking the UMN signs in patients with advanced ALS. For example, the deep tendon reflex is reduced due to severe muscle atrophy. To analyse metabolic changes more directly *in vivo*, high-resolution detection systems for FDG-PET scans and/or a novel disease-specific PET tracer are required.

While the extent ratio was calculated from changed pixel numbers, the Z-score in each pixel was defined based on a significant decrease.
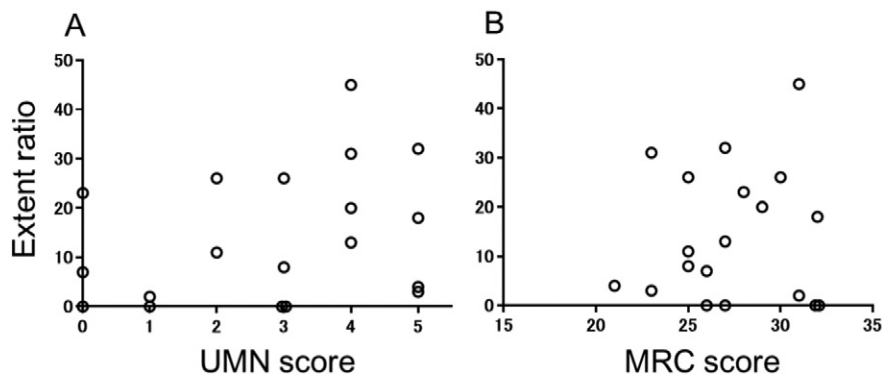
Fig. 5. Scatter plots of extent ratio Z-scores > 1.5 for the symptomatic primary motor cortex regions (the precentral gyrus for upper extremities symptoms or the paracentral lobule for lower extremities symptom) against UMN scores (A) and LMN scores (B). There was no significant correlation.

The extent ratios were therefore regarded as indicators of the glucose metabolic status, and were used to demonstrate the proportion of glucose metabolic changes in the PMC of patients with ALS during disease progression.

The present study has several limitations. First, our study was a retrospective cross-sectional study, and only selected the patient with ALS who underwent FDG-PET scan. Second, in the whole body scan, the brain was scanned only for 2 to 2.5 min. As a result, the total count of brain scans and the image quality of the scans were low. Additionally, the patient group and healthy group were exposed to similar conditions, and we observed a trend; however, different PET scanners were used to analyse these groups, as the control data were acquired from a different study. Our study also involved a small number of patients, no patients presented with bulbar onset, and bulbar signs as following symptom were not evaluated. Finally, our measurement of symptom duration was subjective, and therefore difficult to compare among our cases.

5. Conclusion

In the present study, glucose metabolism in the impaired hemisphere of the PMC decreased depending on the ALS stage, regardless of the UMN clinical signs. These regional changes in the PMC based on FDG-PET assessment might be a novel indicator of the time-dependent course of ALS neurodegeneration.

Funding

Contributors

HE was involved in the conception and design of the study; acquiring, analysing, and interpreting the data; and writing the manuscript. KS contributed to interpreting the data and substantially revising the manuscript. TU, HK, FK, and TT contributed to revising and approving the manuscript.

Competing interests

None.

Acknowledgements

References

[1] L.P. Rowland, How amyotrophic lateral sclerosis got its name: the clinical-pathologic genius of Jeann-Martin Charcot, Arch. Neurol. 58 (2001) 512–515.

[2] J.M. Ravits, A.R. La Spada, ALS motor phenotype heterogeneity, foclity, and spread: deconstructing motor neuron degeneration, Neurology 73 (2009) 805–811.

[3] J. Brettschneider, K. Del Tredici, J.B. Toledo, et al., Stages of pTDP-43 pathology in amyotrophic lateral sclerosis, Ann. Neurol. 74 (2013) 20–38.

[4] T. Nonaka, M. Masuda-Suzukake, T. Arai, et al., Prion-like properties of pathological TDP-43 aggregates from diseased brains, Cell Rep. 4 (2013) 123–134.

[5] T. Sekiguchi, T. Kanouchi, K. Shibuya, et al., Spreading of amyotrophic lateral sclerosis lesions—multifocal hits and local propagation? J. Neurol. Neurosurg. Psychiatry 85 (2014) 85–91.

[6] S. Abrahams, L.H. Goldstein, J.J. Kew, et al., Frontal lobe dysfunction in amyotrophic lateral sclerosis. A PET study, Brain 119 (1996) 2105–2120.

[7] M.O. Habert, L. Lacomblez, P. Maksud, et al., Brain perfusion imaging in amyotrophic lateral sclerosis: extent of cortical changes according to the severity and topography of motor impairment, Amyotroph. Lateral Scler. 8 (2007) 9–15.

[8] M.C. Dalakas, J. Hatazawa, R.A. Brooks, et al., Lowered cerebral glucose utilization in amyotrophic lateral sclerosis, Ann. Neurol. 22 (1987) 580–586.

[9] A. Cistaro, M.C. Valentini, A. Chiò, et al., Brain hypermetabolism in amyotrophic lateral sclerosis: a FDG PET study in ALS of spinal and bulbar onset, Eur. J. Nucl. Med. Mol. Imaging 39 (2012) 251–259.

[10] M. Pagani, A. Chiò, M.C. Valentini, et al., Functional pattern of brain FDG-PET in amyotrophic lateral sclerosis, Neurology 83 (2014) 1067–1074.

[11] B.R. Brooks, R.G. Miller, M. Swash, et al., El Escorial revisited: revised criteria for the diagnosis of amyotrophic lateral sclerosis, Amyotroph. Lateral Scler. Other Motor Neuron Disord. 1 (2000) 293–299.

[12] N.K. Iwata, S. Aoki, S. Okabe, et al., Evaluation of corticospinal tracts in ALS with diffusion tensor MRI and brainstem stimulation, Neurology 70 (2008) 528–532.

[13] J.H. Woo, S. Wang, E.R. Melhem, et al., Linear associations between clinically assessed upper motor neuron disease and diffusion tensor imaging metrics in amyotrophic lateral sclerosis, PLoS One 9 (2014), e105753. .

[14] S. Minoshima, K.A. Frey, R.A. Koeppe, et al., A diagnostic approach in Alzheimer's disease using three-dimensional stereotactic surface projections of fluorine-18-FDG PET, J. Nucl. Med. 36 (1995) 1238–1248.

[15] S. Minoshima, K.L. Berger, K.S. Lee, et al., An automated method for rotational correction and centering of three-dimensional functional brain images, J. Nucl. Med. 33 (1992) 1579–1585.

[16] S. Minoshima, R.A. Koeppe, M.A. Mintun, et al., Automated detection of the intercommissural (AC-PC) line for stereotactic localization of functional brain images, J. Nucl. Med. 34 (1993) 322–329.

[17] S. Minoshima, R.A. Koeppe, K.A. Frey, et al., Anatomical standardization: linear scaling and nonlinear warping of functional brain images, J. Nucl. Med. 35 (1994) 1528–1537.

[18] E. Iseki, N. Murayama, R. Yamamoto, et al., Construction of a (18)F-FDG PET normative database of Japanese healthy elderly subjects and its application to demented and mild cognitive impairment patients, Int. J. Geriatr. Psychiatry 25 (2010) 352–361.

[19] S. Mizumura, S. Kumita, K. Cho, et al., Development of quantitative analysis method for stereotactic brain image: assessment of reduced accumulation in extent and severity using anatomical segmentation, Ann. Nucl. Med. 17 (2003) 289–295.

[20] J.L. Lancaster, M.G. Woldorff, L.M. Parsons, et al., Automated Talairach atlas labels for functional brain mapping, Hum. Brain Mapp. 10 (2000) 120–131.

[21] G.C. Frisoni, M. Bocchetta, G. Chetelat, et al., Imaging markers for Alzheimer disease: which vs how, Neurology 81 (2013) 487–500.

[22] J.J. Kew, P.N. Leigh, E.D. Playford, et al., Cortical function in amyotrophic lateral sclerosis. A positron emission tomography study, Brain 116 (1993) 655–680.

[23] G. Coan, C.S. Mitchell, An assessment of possible neuropathology and clinical relationships in 46 sporadic amyotrophic lateral sclerosis patient autopsies, Neurodegener. Dis. 15 (2015) 301–312.

[24] J. Hatazawa, R.A. Brooks, M.C. Dalakas, et al., Cortical motor-sensory hypometabolism in amyotrophic lateral sclerosis: a PET study, J. Comput. Assist. Tomogr. 12 (1988) 630–636.

[25] Lund and Manchster groups, Clinical and neuropathological criteria for frontotemporal dementia, J. Neurol. Neurosurg. Psychiatry 57 (1994) 416–418.

[26] K. Van Laere, A. Vanhee, J. Verschueren, et al., Value of 18fluorodeoxyglucose-positron-emission tomography in amyotrophic lateral sclerosis: a prospective study, JAMA Neurol. 71 (2014) 553–561.

[27] T.H. Lai, R.S. Liu, B.H. Yang, et al., Cerebral involvement in spinal and bulbar muscular atrophy (Kennedy's disease): a pilot study of PET, J. Neurol. Sci. 335 (2013) 139–144.

[28] H. Adachi, M. Katsuno, M. Minamiyama, et al., Widespread nuclear and cytoplasmic accumulation of mutant androgen receptor in SBMA patients, Brain 128 (2005) 659–670.